

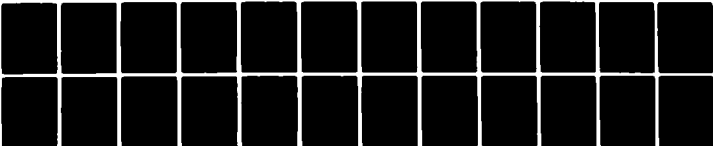
AD-A115 267

SRI INTERNATIONAL MENLO PARK CA F/G 13/13
DYNAMIC ELASTIC-PLASTIC RESPONSE OF BEAMS IN COMBINED THRUST AN--ETC(U)
MAY 82 J D COLTON, J L DEIN, A L FLORENCE DAAG29-79-C-0219
ARO-15400.1-EG NL

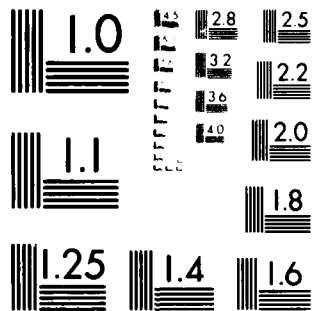
UNCLASSIFIED

[+]

SECRET



END
DATE
FILMED
7 82
DTIC



MICROCOPY RESOLUTION TEST CHART
NATIONAL BUREAU OF STANDARDS 1963-A

(12)

ARO 15400.1-EG

UNCLASSIFIED

SECURITY CLASSIFICATION OF THIS PAGE (When Data Entered)

AD A115267

DTIC FILE COPY

REPORT DOCUMENTATION PAGE		READ INSTRUCTIONS BEFORE COMPLETING FORM
1. REPORT NUMBER	2. GOVT ACCESSION NO.	3. RECIPIENT'S CATALOG NUMBER
4. TITLE (and Subtitle) DYNAMIC ELASTIC-PLASTIC RESPONSE OF BEAMS IN COMBINED THRUST AND BENDING		5. TYPE OF REPORT & PERIOD COVERED Final Report Oct. 16, 1979-Oct. 15, 1981
7. AUTHOR(s) J. D. Colton J. L. Dein A. L. Florence		6. PERFORMING ORG. REPORT NUMBER PYU-1062
9. PERFORMING ORGANIZATION NAME AND ADDRESS SRI International Menlo Park, California 94025		8. CONTRACT OR GRANT NUMBER(s) DAAG29-79-C-0219
11. CONTROLLING OFFICE NAME AND ADDRESS U.S. Army Research Office Post Office Box 12211 Research Triangle Park, NC 27709		10. PROGRAM ELEMENT, PROJECT, TASK AREA & WORK UNIT NUMBERS
14. MONITORING AGENCY NAME & ADDRESS (if different from Controlling Office)		12. REPORT DATE May 15, 1982
		13. NUMBER OF PAGES 31
		15. SECURITY CLASS (of this report) Unclassified
		15a. DECLASSIFICATION/DOWNGRADING SCHEDULE
16. DISTRIBUTION STATEMENT (of this Report) Approved for public release; distribution unlimited.		
17. DISTRIBUTION STATEMENT (of the abstract entered in Block 20, if different from Report) NA		
18. SUPPLEMENTARY NOTES The view, opinions, and/or findings contained in this report are those of the author(s) and should not be construed as an official Department of the Army position, policy, or decision, unless so designated by other documentation.		
19. KEY WORDS (Continue on reverse side if necessary and identify by block number) Long-rod penetrators, elastic-plastic response, structural wave propagation, method of characteristics.		
20. ABSTRACT (Continue on reverse side if necessary and identify by block number) A one-dimensional structural mechanics model is presented for analyzing the elastic-plastic response of rods to slightly inclined end thrusts. The theory is kept simple by restricting the development to cases in which the axial thrust dominates, the bending moment being considered as a perturbation that may grow. Partial unloading of a cross section caused by excessive bending is included in the treatment but requires further numerical study. Solutions are obtained using the method of characteristics. The computer code describing the elastic-plastic wave propagation is simple and may be useful for preliminary design of rod penetrators.		

DTIC ELECTE
JUN 9 1982
S A D

**DYNAMIC ELASTIC-PLASTIC RESPONSE
OF BEAMS IN COMBINED THRUST
AND BENDING**

Final Report

**J. D. Colton
J. L. Dein
A. L. Florence**

May 15, 1982

**Prepared for
U.S. ARMY RESEARCH OFFICE**

Under Contract DAAG29-79-C-0219

**SRI International
Menlo Park, California**

Approved for public release; distribution unlimited

The view, opinions, and/or findings contained in this report are those of the author(s) and should not be construed as an official Department of the Army position, policy, or decision, unless so designated by other documentation.



Accession For	
NTIS GR&I	<input checked="" type="checkbox"/>
DTIC TAB	<input type="checkbox"/>
Unannounced	<input type="checkbox"/>
Justification	
By	
Distribution/	
Availability Codes	
Avail and/or	
Dist Special	

A

STATEMENT OF THE PROBLEM

The response of a long rod penetrator striking armor is of considerable military interest. The complete large-deformation three-dimensional response, including fracture and erosion, is difficult and expensive to model. The problem addressed here was to determine if the part of the projectile behind the tip could be modeled in an approximate way using beam theory.

SUMMARY OF KEY RESULTS

The two most significant results of this research are:

- (1) Development of a theory for treating the thrust-dominated plastic thrust-moment interaction in a beam during loading and partial unloading.
- (2) Insight to the local loading, unloading, and reloading plastic response of a beam loaded axially and transversely at the end.

A theory was developed for modeling the dynamic elastic-plastic response of a beam-column under combined axial and lateral loading. The theory is based on the Timoshenko beam equations and a new formulation for the constitutive relations in the plastic regime. The constitutive relations rely on the simplifying assumption that the state of stress is dominated by the thrust as is the case for long rod penetrators impacting at small angles of attack. This simplifying assumption has three implications: (1) bending, both in loading and unloading at a local cross-section, is treated as a perturbation on the thrust; (2) the degree of work hardening at a given cross section depends only on the thrust at that cross section; and (3) the plastic shear strain can be neglected.

The analysis is based on the Timoshenko beam equations. For elastic response, the thrust-longitudinal strain and moment-curvature relationships are linear and uncoupled. For plastic response during

loading and unloading over a portion of the cross section (partial unloading), the resultant thrust and moment at that cross section are coupled. These resultants are found by applying the appropriate stress-strain relation (elastic or plastic) at each point of the cross section and integrating over the cross-sectional area. A single parameter can be used to specify the location of the boundary between the elastic and plastic regions. This approach was used to formulate the stress-strain relations for loading and partial unloading, both of which are dominated by thrust. The equations were solved by the method of characteristics.

We attempted to calculate the response of a penetrator-type beam under a predominantly axial end load such that the dominant loading due to thrust would be accompanied by partial unloading due to bending. For small values of the angle between the direction of the resultant load and the beam axis only loading, predominantly axial with small bending, was produced. As this angle increased to values as small as 8 degrees, partial unloading caused by the increased bending was produced over a portion of the length of the rod. However, this portion soon became reloaded.

We were unable to generate partial unloading at any location without significant reloading. We attribute this effect to the fact that partial unloading occurs along a steeper slope of the stress-strain curve than the slope for plastic loading. Therefore, as unloading takes place there is an increase in the effective local beam stiffness resisting the superposed bending. This disturbance propagates away from the initial point of partial unloading and causes reloading at nearby points.

We conclude that any model of penetrator response must include at least one cycle of loading, partial unloading and, reloading.

PUBLICATIONS PUBLISHED

One paper has been submitted for publication in the International Journal of Solids and Structures:

"DYNAMIC ELASTIC-PLASTIC RESPONSE OF BEAMS IN COMBINED THRUST AND BENDING" by J. D. Colton, J. L. Dein, and A. L. Florence

SCIENTIFIC PERSONNEL

The following persons participated in this research:

1. J. D. Colton
2. J. L. Dein
3. A. L. Florence

No additional advanced degrees were earned by any persons participating in this research project.

BIBLIOGRAPHY

1. S. Timoshenko. *Vibration Problems in Engineering*. D. Van Nostrand Company, Inc. (1955).
2. R. Courant and D. Hilbert. *Methods of Mathematical Physics*. Vol. 2, Interscience (1962).
3. J. D. Colton. *Structural Response of Earth Penetration in Angle-of-Attack Impacts*. *Shock and Vibration Bulletin*, 48(2), September 1978.
4. S. Ranganath and R. J. Clifton. *Normal Impact of an Infinite Elastic-Plastic Beam by a Semi-Infinite Elastic Rod*. *Int. J. Solids Structures*, 8, 41-67 (1972).
5. R. D. Mindlin. *Influence of Rotatory Inertia and Shear on Flexural Motions of Isotropic Elastic Plates*. *J. Appl. Mech.*, 18, 31-38 (1951).
6. R. D. Mindlin and H. Deresiewicz. *Timoshenko's Shear Coefficient for Flexural Vibrations of Beams*. *J. Appl. Mech.*, 22, 175-178 (1955).

7. D. C. Erlich, R. D. Caligiuri, and J. H. Giovanola. Computational Model for Armor Penetration. SRI Progress Report 26 to Ballistics Research Laboratory under Contract DAAK11-78-C-0115 (1981).

APPENDIX

Paper submitted for publication in the International Journal of
Solids and Structures.

**DYNAMIC ELASTIC-PLASTIC RESPONSE OF
BEAMS IN COMBINED THRUST AND BENDING†**

by

J. D. Colton, J. L. Dein, and A. L. Florence
Poulter Laboratory
SRI International
Menlo Park, California 94025

†Supported by the U.S. Army Research Office.

ABSTRACT

A one-dimensional structural mechanics model is presented for analyzing the elastic-plastic response of rods to slightly inclined end thrusts. The theory is kept simple by restricting the development to cases in which the axial thrust dominates, the bending moment being considered as a perturbation that may grow. Partial unloading of a cross section caused by excessive bending is included in the treatment but requires further numerical study. Solutions are obtained using the method of characteristics. The computer code describing the elastic-plastic wave propagation is simple and may be useful for preliminary design of rod penetrators.

1. INTRODUCTION

Long-rod penetrators for defeating armor have been extensively analyzed by finite-difference computer codes to obtain their axisymmetric elastic-plastic response to impact. If the end loads result in stress waves that are not axisymmetric, the continuum code solutions become three-dimensional and complex. As an aid to preliminary analyses of rods, we present a one-dimensional structural mechanics approach that is suitable for treating elastic-plastic wave propagation along rods for cases involving small departures from axisymmetry.

In this simple theory, we assume that plane cross sections of the rod always remain plane, which allows us to formulate the problem in terms of the axial and transverse velocities of the center of the circular cross section, the angular velocity of the planar cross section about the appropriate diameter, and the stress resultants consisting of the thrust, bending moment, and shear force acting on the section. The derivation of the governing equations is based on the Timoshenko theory of beams [1]. This well-known theory takes into account rotary inertia and overall shear distortion of a beam element. However, our main reason for using this theory as a basis is that the resulting equations are hyperbolic and lend themselves to solution by the method of characteristics [2].

Colton [3] has used this structural mechanics approach to analyze the elastic response of earth penetrators, which may be considered long rods. Good agreement was found between predicted and experimental strains. Ranganath and Clifton [4] have also used this approach successfully to analyze the elastic-plastic response of an infinite beam to transverse impact.

We have intentionally restricted the theory so that the axial thrust is supposed to dominate the bending moment. The axially applied end load monotonically increases and it is kept at a small angle of inclination to the rod axis. It is also assumed that the shear force

does not participate in the yield condition. These restrictions allow us to assess the usefulness of the elastic-plastic theory in its simplest form, after which the effects of relaxing restrictions can be studied.

Figure 1 illustrates the effect of a dominant thrust with the bending moment regarded as a perturbation that can grow. Figure 1a shows the end thrust N_0 inclined at a small angle α to the rod axis. Let ACB be a cross section of the rod where A and B are the top and bottom fibers and C is the fiber on the horizontal diameter or mid-plane. If the curvature at the section has its concave side on top, the compressive strain at A is larger than the compressive strain at C while the strain at B is smaller than the strain at C. Also, while loading increases, all strains increase provided the thrust dominates. The stress-strain states at A, C, and B are shown in Fig. 1b, with the attached arrows indicating that the strains are increasing. At B, the bending that is causing the stress-strain state to lag behind may grow enough to cause strain-rate reversal, in which case partial unloading of the cross section occurs. This eventuality is in fact included in the theoretical development of the next section, in an attempt to prepare for extension of the simplest form of the elastic-plastic theory. It is also included to show how partial unloading introduces new wave velocities, as in the work of Ranganath and Clifton [4].

2. GOVERNING EQUATIONS

Figure 2a shows a rod element with its attendant axial force, shear force, and bending moment, which at an axial position x are represented by N , Q , and M . Figure 2b shows the axial and transverse displacements, ξ and η , the rotation ϕ , and element overall shear strain γ , all at location x . Thus, the three equations of motion may be written as

$$N_x = \rho A \xi_{tt} \quad (2.1a)$$

$$M_x + Q = \rho I \phi_{tt} \quad (2.1b)$$

$$Q_x = \rho A \eta_{tt} \quad (2.1c)$$

where ρ is the density of the rod material, $A = \pi a^2$ is the cross-sectional area, and $I = \pi a^4/4$ is the second moment of area. Subscripts x and t denote partial differentiation.

Because we assume that the shear strains remain elastic, we may take

$$Q = k' A G \gamma \quad (2.2a)$$

where k' is the cross section shear coefficient [5] and G is the modulus of rigidity. For a circular cross section, we take $k' = 0.827$ [6]. In terms of the rod element slope and rotation, the section shear strain is

$$\gamma = \eta_x - \phi \quad (2.3a)$$

When the compressive strains are increasing over the entire cross section, as shown in Fig. 1b, the incremental forms for the generalized stress-strain relationships are

$$N_t = H A \epsilon_t \quad (2.4a)$$

$$M_t = H I \kappa_t \quad (2.4b)$$

where $\epsilon = \xi_x$ is the cross section midsurface strain and $\kappa = \phi_x$ is the curvature of the rod element. The modulus $H(\epsilon)$ is a constant only when the strain is less than the yield strain, the case when H becomes Young's modulus E .

In terms of the axial, transverse, and angular velocities u , v , and ω given by

$$u = \xi_t \quad v = \eta_t \quad \omega = \phi_t \quad (2.5a)$$

equations (2.1a), (2.1b), (2.1c), (2.2a), (2.4a), and (2.4b) can be put in the form

$$\begin{aligned}
 \rho A u_t - N_x &= 0 \\
 N_t - H A u_x &= 0 \\
 \rho I \omega_t - M_x &= Q \\
 M_t - H I \omega_x &= 0 \\
 \rho A v_t - Q_x &= 0 \\
 Q_t - k' A G v_x &= -k' A G \omega
 \end{aligned} \tag{2.6a}$$

To allow the theory to treat the case of partial unloading, which starts with the onset of strain-rate reversal at the convex outer fiber (at $z = a$ when $d\kappa > 0$), consider the strain and stress increment distributions in Fig. 3 for $d\kappa > 0$ associated with a time increment dt . Strain rate reversal occurs in the region $-a < z < z_1$, so elastic unloading occurs there. From Fig. 3a showing the strain increments, we have

$$d\epsilon = d\epsilon_0 + z d\kappa \tag{2.7a}$$

When we set $d\epsilon = 0$, equation (2.1a) determines the value z_1 that divides the cross section into loading and unloading regions. In terms of velocities

$$z_1 = -u_x / \omega_x \tag{2.8a}$$

From Fig. 3b showing the stress increments, we have

$$d\sigma = \begin{cases} H d\epsilon & z_1 < z < a \\ E d\epsilon & -a < z < z_1 \end{cases} \tag{2.9a}$$

By integrating (2.9a) with ds given by (2.7a) over the rod cross section, we can obtain the incremental thrust and bending moment in the form

$$N_t = H_0 A u_x + H_1 \sqrt{A I} \omega_x \quad (2.10a)$$

$$M_t = H_1 \sqrt{A I} u_x + H_2 I \omega_x \quad (2.10b)$$

where

$$H_0 = H + (E - H)i_0$$

$$H_1 = (E - H)i_1$$

$$H_2 = H + (E - H)i_2 \quad (2.10c)$$

$$i_0 = \frac{1}{A} \int_{-a}^{z_1} b \, dz$$

$$i_1 = \frac{1}{\sqrt{A I}} \int_{-a}^{z_1} bz \, dz$$

$$i_2 = \frac{1}{I} \int_{-a}^{z_1} bz^2 \, dz \quad -a \leq z_1 \leq a \quad \kappa_t > 0 \quad (2.10d)$$

when $\kappa_t < 0$, the thrust and moment rates are still given by (2.10a) and (2.10b) provided we change the lower and upper integration limits in (2.10d) to z_1 and a . For a circular cross section, we have $b = 2(a^2 - z^2)^{1/2}$ so the integrals in (2.10d) become

$$i_0 = \frac{1}{\pi} (\phi_1 - \frac{1}{2} \sin 2\phi_1)$$

$$i_1 = -\frac{4}{3\pi} \sin^3 \phi_1$$

$$i_2 = \frac{1}{\pi} (\phi_1 - \frac{1}{4} \sin 4\phi_1) \quad \kappa_t > 0 \quad (2.11a)$$

where

$$\cos \phi_1 = -z_1/a \quad 0 \leq \phi_1 \leq \pi \quad (2.11b)$$

When $\kappa_t < 0$, we replace i_0 , i_1 , and i_2 by j_0 , j_1 , and j_2 where

$$j_0 = 1 - i_0 \quad j_1 = -i_1 \quad j_2 = 1 - i_2 \quad (2.12a)$$

In Fig. 3a ($\kappa_t > 0$), we see that partial unloading starts when $z_1 = -a$, so whenever $z \leq -a$ the integrals are set equal to zero. In these cases (2.10c) gives $H_0 = H$, $H_1 = 0$, $H_2 = H$ so the thrust and moment rates (2.10a) and (2.10b) reduce to (2.4a) and (2.4b) for the fully loading section. If partial unloading continues with z_1 monotonically increasing until it reaches the value $z_1 = a$, we reach the stage of fully elastic unloading. When $z_1 = a$, we have $i_0 = 1$, $i_1 = 0$, and $i_2 = 1$ from (2.10d) and consequently $H_0 = E$, $H_1 = 0$, and $H_2 = E$ from (2.10c). Then the thrust and moment rates reduce to (2.4a) and (2.4b) with H taking the special constant value E .

The governing equations that include monotonic partial unloading are the set (2.6a) with the thrust and moment rate equations replaced by the more general forms (2.10a) and (2.10b). In matrix form, we have

$$A w_t + B w_x = C w \quad (2.13a)$$

in which

$$w = \begin{bmatrix} u \\ N \\ \omega \\ M \\ v \\ Q \end{bmatrix} \quad A = \begin{bmatrix} \rho A & 0 & 0 & 0 & 0 & 0 \\ 0 & 1 & 0 & 0 & 0 & 0 \\ 0 & 0 & \rho I & 0 & 0 & 0 \\ 0 & 0 & 0 & 1 & 0 & 0 \\ 0 & 0 & 0 & 0 & \rho A & 0 \\ 0 & 0 & 0 & 0 & 0 & 1 \end{bmatrix}$$

$$B = \begin{bmatrix} 0 & -1 & 0 & 0 & 0 & 0 \\ -H_0 A & 0 & -H_1 A I & 0 & 0 & 0 \\ 0 & 0 & 0 & -1 & 0 & 0 \\ -H_1 A I & 0 & -H_2 I & 0 & 0 & 0 \\ 0 & 0 & 0 & 0 & 0 & -1 \\ 0 & 0 & 0 & 0 & -k'AG & 0 \end{bmatrix} \quad C = \begin{bmatrix} 0 & 0 & 0 & 0 & 0 & 0 \\ 0 & 0 & 0 & 0 & 0 & 0 \\ 0 & 0 & 0 & 0 & 0 & 1 \\ 0 & 0 & 0 & 0 & 0 & 0 \\ 0 & 0 & 0 & 0 & 0 & 0 \\ 0 & 0 & -k'AG & 0 & 0 & 0 \end{bmatrix}$$

3. CHARACTERISTIC PROPERTIES OF THE EQUATIONS

The governing equations (2.13a) form a system of quasi-linear hyperbolic equations of first order (2.1b). The characteristic velocities are the six roots of the characteristic equation

$$|A^{-1} B - c| = 0 \quad (3.1a)$$

Expanding the determinant (3.1a) leads to

$$[(\rho c^2)^2 - (H_0 + H_2)\rho c^2 + (H_0 H_2 - H_1^2)](\rho c^2 - k'G) = 0 \quad (3.2a)$$

which has as roots the six wave velocities

$$c_f = \pm \left(\frac{1}{2\rho}\right)^{1/2} \left\{ H_0 + H_2 + \left[(H_0 - H_2)^2 + 4H_1^2 \right]^{1/2} \right\}^{1/2} \quad (3.2b)$$

$$c_s = \pm \left(\frac{1}{2\rho}\right)^{1/2} \left\{ H_0 + H_2 - \left[(H_0 - H_2)^2 + 4H_1^2 \right]^{1/2} \right\}^{1/2} \quad (3.2c)$$

$$c_q = \pm \left(\frac{k'G}{\rho}\right)^{1/2} \quad (3.2d)$$

The fast and slow wave speeds, c_f and c_s of (3.2b) and (3.2c) govern the propagation of the thrust and moment in both directions along the rod. The wave speed c_q given by (3.2d) governs the propagation of shear.

Wave velocities associated with a fully loaded cross section are found by setting $H_0 = H_2 = H$ and $H_1 = 0$ in (3.2b) and (3.2c). These substitutions give

$$c_f = c_s = c = (H/\rho)^{1/2} \quad (3.3a)$$

If we determine the left null row vector λ_1 of the characteristic matrix containing the corresponding characteristic value c_1 , that is, if we solve

$$\lambda_1 (A^{-1}B - c_1 I) = 0$$

we find the characteristic equations from

$$\lambda_1 (w_t + c_1 w_x) = \lambda_1 A^{-1} C w \quad (3.4a)$$

Following this procedure leads to the set of equations

$$\rho c_f A R_f du + R_f dN + \rho c_f I d\omega + dM = c_f Q dt$$

along $\frac{dx}{dt} = \pm c_f$

$$\rho c_s A R_s du + R_s dN + \rho c_s I d\omega + dM = c_s Q dt$$

along $\frac{dx}{dt} = \pm c_s$

$$\rho c_q A dv + dQ = \pm k' A G \omega dt$$

along $\frac{dx}{dt} = \pm c_q \quad (3.5a)$

where

$$R_f = \frac{H_1 (I/A)^{1/2}}{\rho c_f^2 - H_0} \quad R_s = \frac{H_1 (I/A)^{1/2}}{\rho c_s^2 - H_0} \quad (3.5b)$$

Characteristic equations associated with a fully loaded cross section are found by setting $H_0 = H_2 = H$ and $H_1 = 0$ in the governing equations (2.13a) finding the roots (3.2d) and (3.3a) of the resultant determinant (3.1a), and hence the resultant null left row vectors of the characteristic matrix for use in (3.4a). Another procedure is to find the limits of (3.5b). The values of R_f and R_s tend to different limits as c_f and c_s tend to c . Hence the equations along the characteristics become

$$\rho c A \, du + dN = 0$$

$$\rho c I \, d\omega + dM = c Q \, dt$$

$$\text{along } \frac{dx}{dt} = \pm c$$

$$\rho c_q A \, d_v + dQ = \pm k' A G \omega \, dt \quad (3.6a)$$

$$\text{along } \frac{dx}{dt} = \pm c_q$$

4. NUMERICAL SCHEME

To integrate the appropriate form of the characteristic equation (3.5a) along the characteristics, we first chose a rectangular mesh in the x - t plane consisting of intersections of the lines $x = (i - 1)\Delta x$ and $t = (j - 1)\Delta t$ for $i = 1, 2, \dots$ and $j = 1, 2, \dots$. We then adopted a scheme for finding the values of the dependent variables at the mesh points P along the line $t = t_{j+1}$ from values Q already determined along line $t = t_j$. Figure 4 shows typical cells with linear segments of the backward and forward characteristics required to determine values at P from the values of $Q_-, Q,$ and Q_+ by solving the finite difference form of

equations (3.5a). The cell size was determined by the elastic velocity, that is, $dx/dt = c$ where $c = (E/\rho)^{1/2}$. The values along the line $t = t_j$ at the points of intersection with the characteristics from P were obtained from the mesh point values at Q_- , Q, and Q_+ by linear interpolation, the initial slopes c_f and c_g of the plastic wave characteristics from P being approximated by those at Q. After solving the finite-difference form of the characteristic equations (3.5a) to obtain the first estimate of the values at P, the dependent variable values at the midpoints of the characteristic segments were used to adjust the slopes for a second iteration. At each time step, z_1 from (2.8a) was calculated to determine the local loading state and hence the appropriate form of the characteristic equation could be selected. If reloading was detected by a reversal of the monotonic progress of z_1 , the calculations were terminated because the theory does not treat this case.

5. NUMERICAL EXAMPLES

Calculations were performed for a rod having a radius of 1 cm, and a length of 20 cm. We used the simplified stress-strain relationship shown by the curve in Figure 5. The curve consists of a linear elastic part smoothly joined to a linear work hardening part, and it is based on a static tension test on uranium containing 3/4% titanium [7]. The corresponding value of the material properties are:

Young's modulus	$E = 160 \text{ GPa}$
shear modulus	$G = 59.3 \text{ GPa (using } \nu = 0.35)$
hardening modulus	$H = 35 \text{ GPa}$
yield stress	$\sigma_y = 730 \text{ MPa}$
density	$\rho = 18.1 \text{ g/cm}^3$.

We used the bilinear loading history of Fig. 6 at one end of the rod while maintaining the other end free of loading. Pure thrust loading gives yielding at $N_y = 2.3 \times 10^5 \text{ N}$. This loading history was chosen in

a simple form, suitable for evaluating the performance of the calculational procedure, rather than in a form based on experimental or continuum mechanics codes results. Also, performance evaluation was restricted to the initial wave transit.

Before generating results for the complete rod problem, we compared the results generated by our computer program with the analytic results for the case of pure elastic-plastic thrust (normal incidence). In the computer code, the bilinear stress-strain curve between points 1 and 2 in Fig. 5 was replaced by a smooth curve. In the analysis, this region was replaced by a straight line. For this problem, a ramp loading of 0.786×10^5 N/ μ sec was applied. Figure 7 shows the distributions of thrust along the rod when the applied thrust has reached 2.3 times the yield thrust, N_y . For excellent agreement, the code curve should pass through point 2 as well as point 1. Because of the different representations of the stress-strain curve between points 1 and 2 in Fig. 5, the solutions are different between these points in Fig. 7. The plastic wave from the loaded end should pass through point 2. However, propagation appears faster than it should because the interpolation procedure is performed out within an x-t mesh sized for the elastic wave propagation. Figure 7 gives a qualitative measure of the error involved.

A similar comparison was made for propagation of bending moments. A ramp shear load was applied at one end of the rod and the code, with the yield stress set to zero, was arranged to produce plastic moment propagation within an x-t mesh sized for elastic wave propagation along $dx/dt = (E/\rho)^{1/2}$. The result was compared with elastic wave propagation by changing the mesh size to $dx/dt = (H/\rho)^{1/2}$. A comparison of the moment distributions along the rod is provided by Fig. 8. The effect of the interpolation for plastic waves with an elastic wave mesh is seen with the solid line. It indicates that a signal is being allowed to propagate faster than its true velocity, as in the case of plastic thrust (Fig. 7).

Figure 9 shows the distributions of the thrust and moment along the rod when the elastic wave has traversed the entire length of the rod (20 cm). The stress-strain curve is that of Fig. 5 and the thrust loading, applied at an angle of 2° to the rod axis, is that of Fig. 6. We see that a bending moment is developing near the loaded end, so under the ideal loading conditions of this example the end could soon break off.

In this example, the code operated in a simple mode with fully elastic-plastic loading throughout. Similar examples at larger angles of attack ($\sim 8^\circ$) cause partial unloading of the rod cross section, but for the few examples investigated this partial unloading was soon followed by reloading, for which the code mechanics do not apply. Partial unloading increases the section bending stiffness and hence the resistance to the bending moment. Associated with this increased stiffness is an increased wave velocity, so that neighboring sections become influenced. Further work is needed to define the limits of applicability of the program in terms of the problem parameters, such as angle of attack.

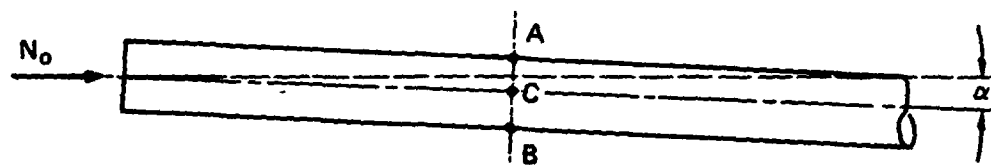
6. CONCLUSIONS

Our main conclusion is that the structural mechanics formulation works well for analyzing the elastic-plastic response of rods under thrust loadings inclined at small angles to the rod axis. The angles allowable will depend on other parameters such as rod radius, but if the bending moment is stimulated as a growing perturbation on the thrust, useful results will be obtained by a simple computer code.

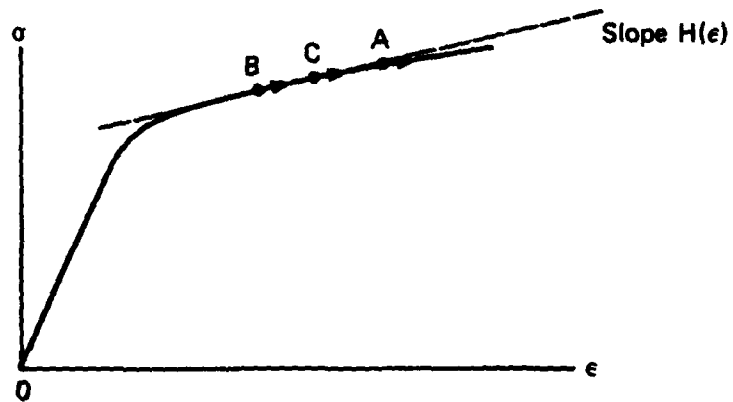
Further numerical investigations are needed to extend the code so that useful results may be obtained when partial unloading occurs. Our examples indicate that partial unloading is rapidly followed by reloading. Reloading requires monitoring of the strain history and introduces a complication that would remove the advantage of simplicity relative to a finite-difference code.

REFERENCES

- [1] S. TIMOSHENKO, Vibration Problems in Engineering. D. Van Nostrand Company, Inc. (1955).
- [2] R. COURANT and D. HILBERT, Methods of Mathematical Physics. Vol. 2. Interscience (1962).
- [3] J. D. COLTON. Structural response of earth penetrators in angle-of-attack impacts. Shock and vibration bulletin, 48, Part 2 (September 1978).
- [4] S. RANGANATH and R. J. CLIFTON. Normal impact of an infinite elastic-plastic beam by a semi-infinite elastic rod. Int. J. Solids Structures, 8, 41-67 (1972).
- [5] R. D. MINDLIN. Influence of rotatory inertia and shear on flexural motions of isotropic elastic plates. J. Appl. Mech., 18, 31-38 (1951).
- [6] R. D. MINDLIN and H. DERESIEWICZ. Timoshenko's shear coefficient for flexural vibrations of beams. J. Appl. Mech., 22, 175-178 (1955).
- [7] D. C. ERLICH, R. D. CALIGIURI, and J. H. GIOVANOLA. Computational model for armor penetration. SRI Progress Report 26 to Ballistics Research Laboratory under contract DAAK11-78-C-0115 (1981).



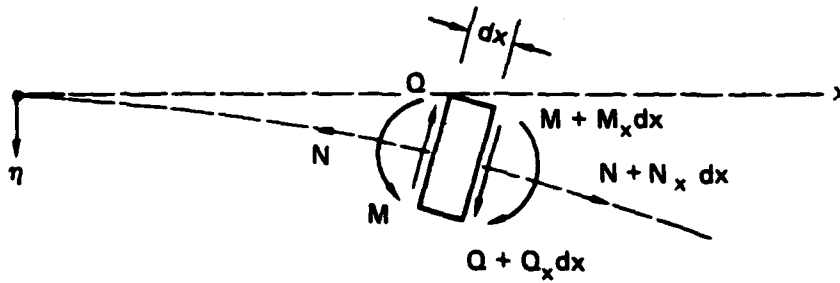
(a) Penetrator under almost normal impact



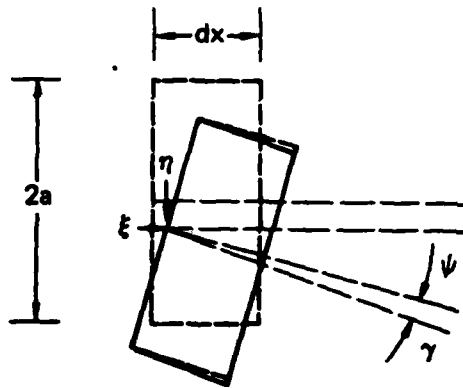
(b) Compressive stress-strain curve

JA-1082-4

FIGURE 1 ROD CROSS SECTION STRESS-STRAIN STATES DURING LOADING



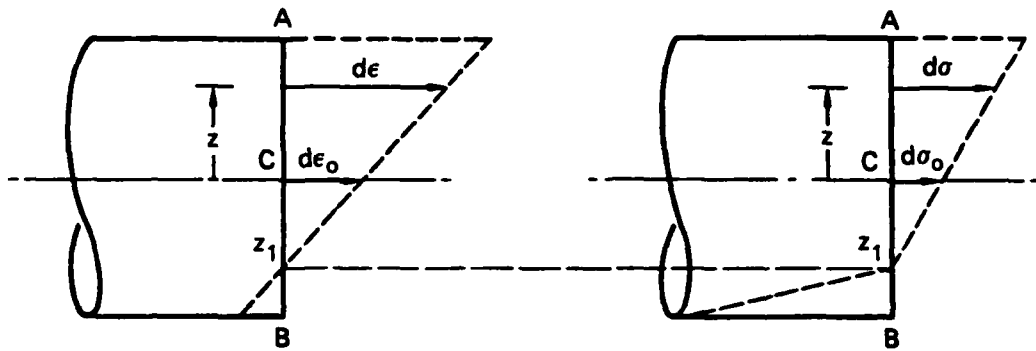
(a) Resultant forces and moments on a rod element



(b) Kinematics of a rod element

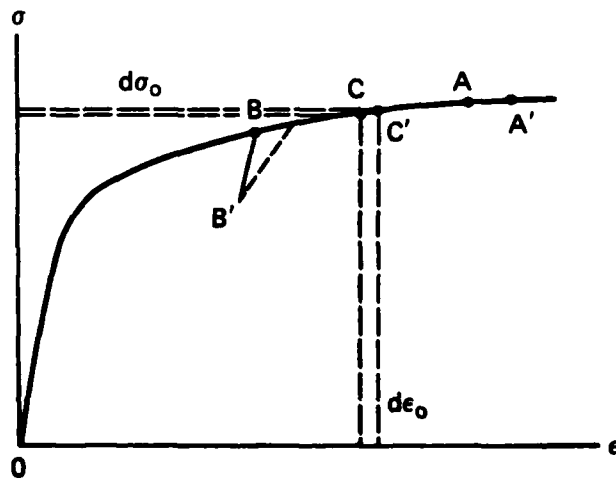
JA-1082-6

FIGURE 2 GENERALIZED FORCES AND DISPLACEMENTS FOR A ROD ELEMENT
 (Sign convention: all quantities shown positive)



(a) Strain increments

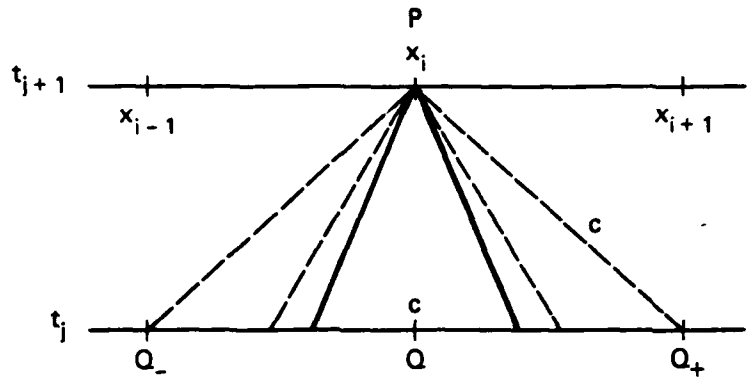
(b) Stress increments



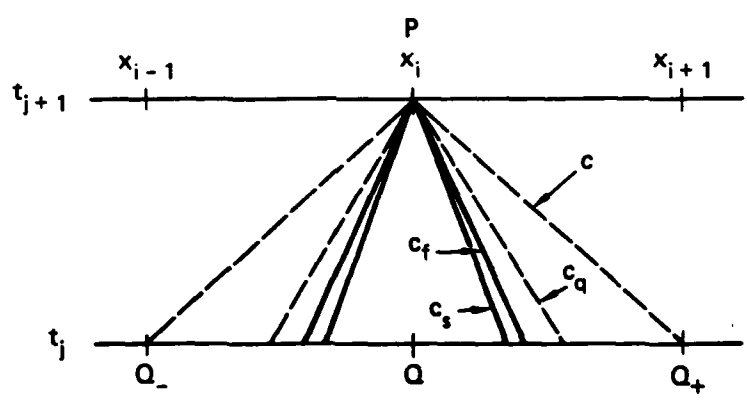
(c) Stress-strain states

JA-1082-8

FIGURE 3 PARTIAL UNLOADING (Case $dx > 0$)



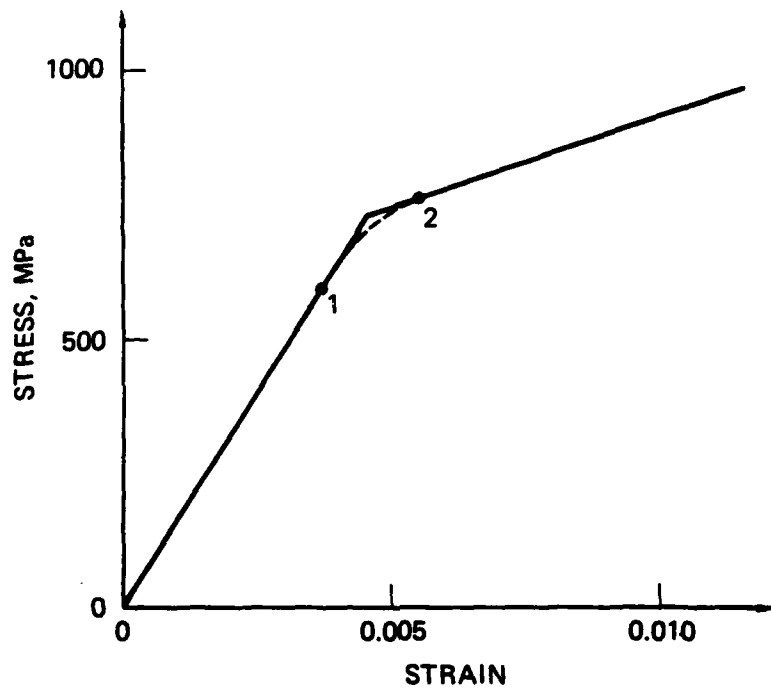
(a) Full elastic-plastic loading



(b) Partial unloading

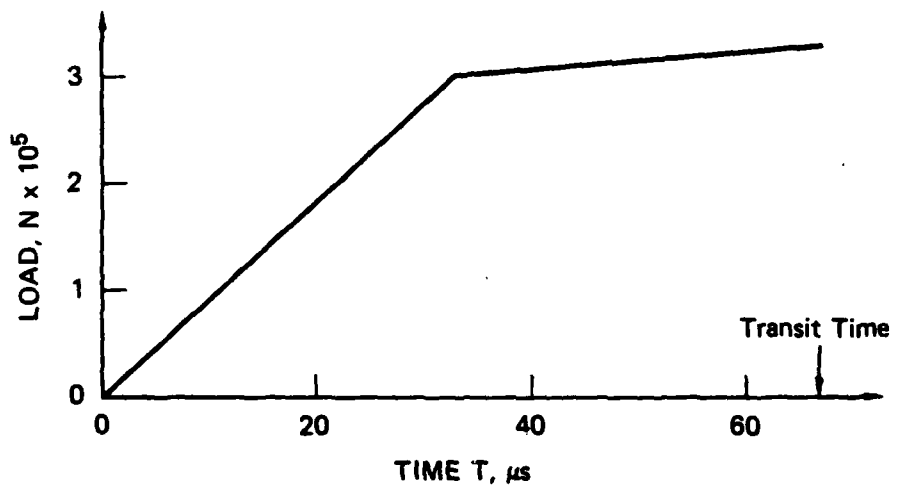
JA-1082-7

FIGURE 4 CHARACTERISTIC CURVES AND MESH POINTS



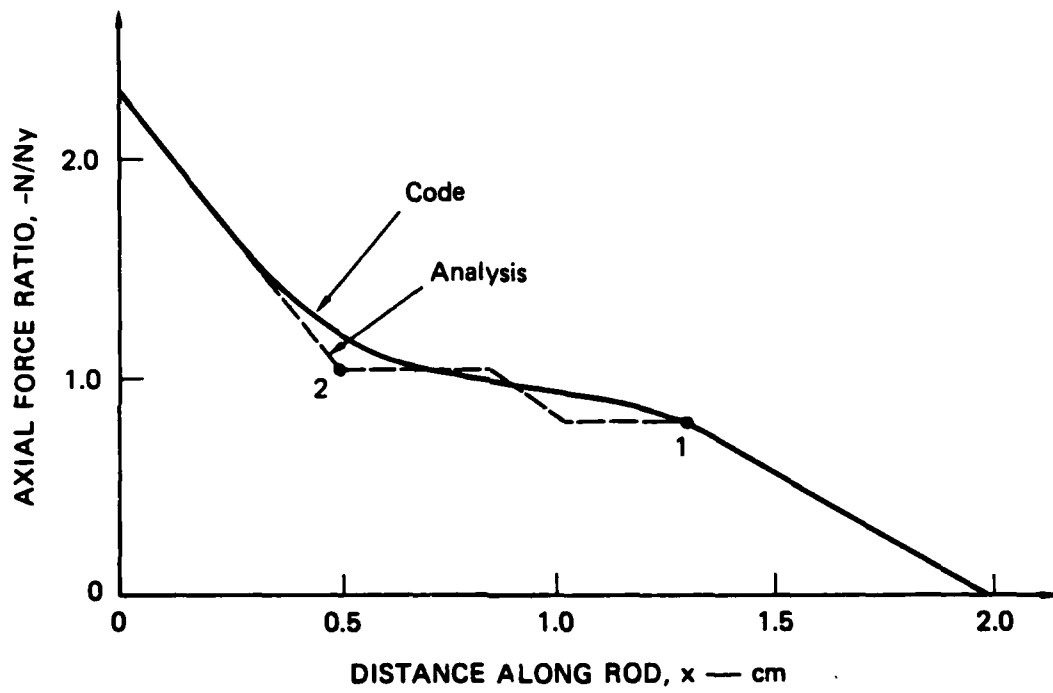
JA-1062-8

FIGURE 5 STRESS-STRAIN RELATIONSHIP USED IN ROD CALCULATIONS



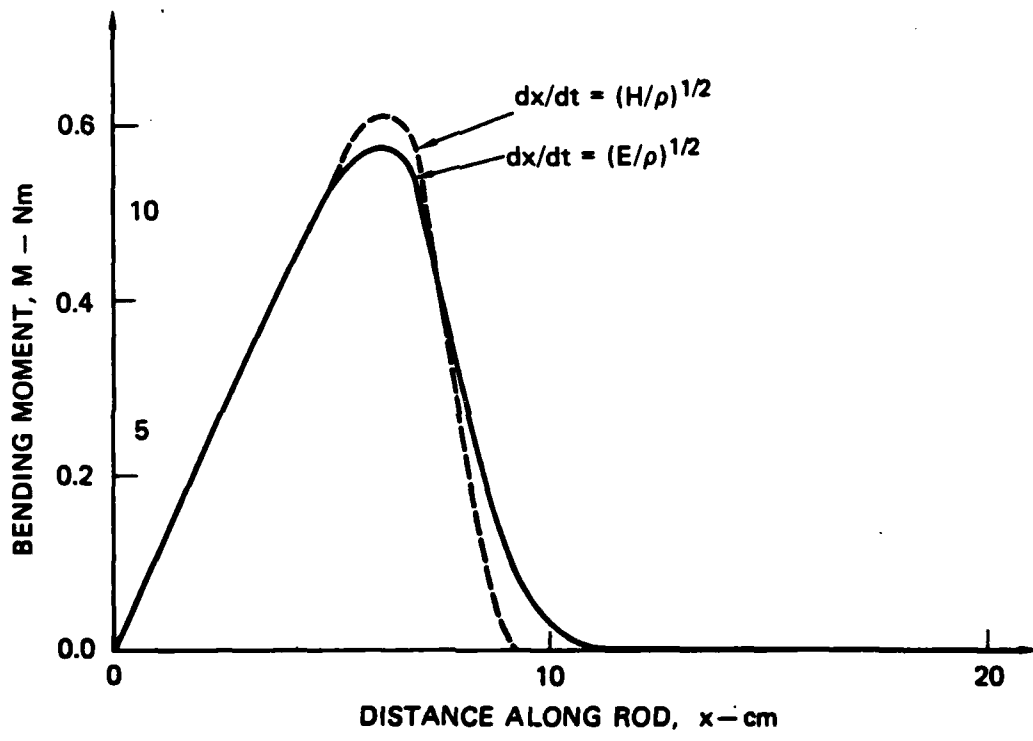
JA-1082-0

FIGURE 6 BILINEAR LOADING FUNCTION



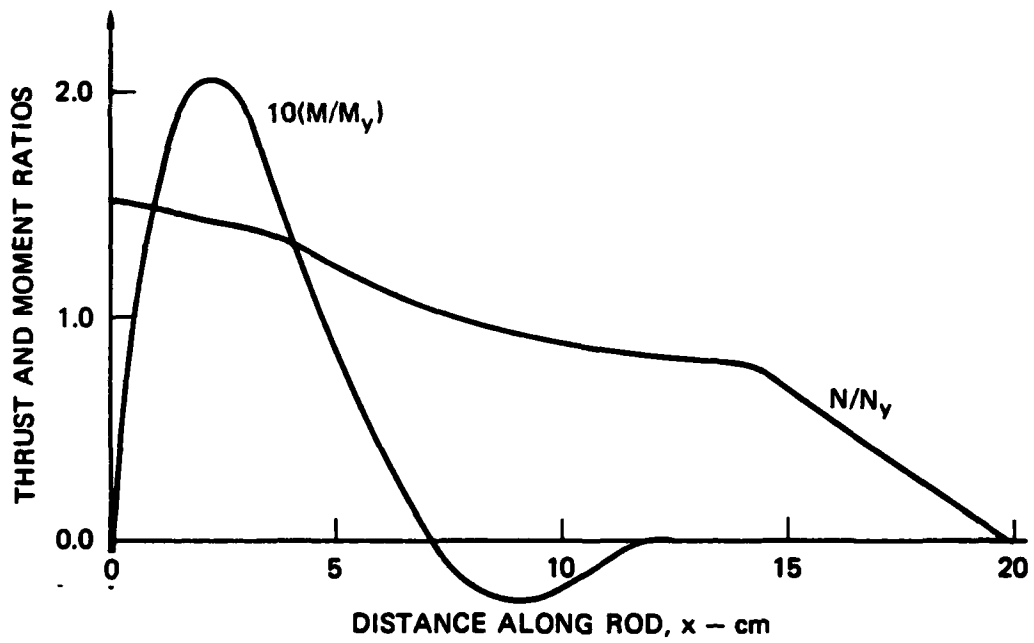
JA-1062-10

FIGURE 7 COMPARISON OF THRUST RATIOS FROM ANALYSIS AND COMPUTER PROGRAM



JA-1062-11

FIGURE 8 DISTORTION OF PLASTIC MOMENT DUE TO ELASTIC CELL SIZE



JA-1062-12

FIGURE 9 THRUST AND MOMENT DISTRIBUTIONS AT ELASTIC WAVE TRANSIT TIME

DATE
ILMEI
— 8